3.6.2

Reflection of slow neutrons from powder of nanorods

V K Ignatovich[1] and V V Nesvizhevsky[2]

[1] Joint Institute for Nuclear Research, 6 Joliot-Curie, Dubna 141980 Russia
[2] Institut Max von Laue - Paul Langevin, 71 avenue des Martyrs F-38042 Grenoble Cedex 9 France

E-mail: v.ignatovi@gmail.com, nesvizhevsky@ill.eu

Abstract. Two phenomena were recently observed: efficient diffuse reflection of very cold neutrons (VCN) from nano-structured matter for any angle of neutron incidence to the matter surface, and also quasi-specular reflection of cold neutrons (CN) from nano-structured matter for small angles of neutron incidence to the matter surface. In both cases, powder of diamond nanoparticles was used as nano-structured matter, and the measured reflection probabilities by far exceeded the values known for alternative reflectors. Both these phenomena are already used in neutron experiments and for building neutron sources. In the present theoretical work, we consider an option of further increasing the efficiency of nano-structured reflectors due to replacing spherical nanoparticles by nanorods. We showed that VCN albedo from powder of randomly oriented nanorods is lower than their albedo from powder of nanospheres of equal diameter. However albedo of VCN and quasi-specular reflection of CN from powder of long nanorods oriented parallel to the powder surface exceed those for powder of nanospheres of equal diameter.

1. Introduction

Efficient neutron reflectors are needed in experiments as well as for building neutron sources. For ultracold neutrons (UCN) [1-3] ($E < u \approx 10^{-7}$ eV), neutron optical potential of matter u is nearly the ideal reflector, which provides the probability of specular reflection close to unity, at any temperature of matter and at any incidence angle. Neutrons of higher energy E also can be totally specularly reflected from mirrors but only at small grazing angles, smaller than some critical angle $\theta_c \approx \sqrt{u/E}$ different for different materials. To increase the critical angle, say, n times, supermirrors M(n) are produced, which are multi-layers composed of bilayers of two substances with different optical potentials. The thickness of bilayers are gradually changing from one bilayer to the next one according to some law [4]. In this way the best mirror M(6.7) was produced in Japan [5]. It contains 4000 bilayers. Such a supermirror, which though provides almost 20% reflectivity at $\theta = \theta_c$, nevertheless gives not only specular, but also large fraction of nonspecular diffuse reflection. It happens because of large interlayer roughnesses appearing as a result of incommensurability of layer thicknesses and interatomic distances. It is possible to overcome this defect by using periodic chains of bilayers as reported in [6]. This algorithm had not yet been technologically realized.

Until recently, efficient reflectors of neutrons with the energy of up to $10^{-2(3)}$ eV had not been known. At the energy of $\sim 10^{-2}$ eV, neutron wavelength is comparable with inter-atomic distances thus effects of elastic diffraction and diffuse reflection in respectively ordered and

disordered matter appear. At even larger energies, inelastic processes, which provide moderation and reflection of neutrons in nuclear reactors [7], prevail.

Two phenomena were observed recently: efficient diffuse reflection of very cold neutrons (VCN) from nano-structured matter for any angle of neutron incidence to the matter surface, and also quasi-specular reflection of cold neutrons (CN) from nano-structured matter for small angles of neutron incidence to the matter surface [8-15]. In both cases, powder of diamond nanoparticles was used as nano-structured matter, and the measured reflection probabilities by far exceeded the values for known alternative reflectors. Both these phenomena are already used in neutron experiments and for building neutron sources. In the present theoretical work, we consider an option of further increasing the efficiency of nano-structured reflectors replacing spherical nanoparticles by nanorods. To be specific, we choose two values of neutron velocity: 1) 50 m/s, as nano-structured reflectors are very efficient at this neutron velocity, and 2) 450 m/s, as, on one hand, the efficiency of nano-structured reflectors made of nanospheres rapidly decreases at this neutron velocity and, on another hand, such reflectors are highly requested, for instance, for increasing UCN density in UCN sources based on superfluid helium [16, 17], used in particular for the GRANIT spectrometer [18], aiming at studies of/with quantum states of neutrons in gravitational and centrifugal potentials [19, 20], [21-23]. If optical potential of a nanorod material is much smaller than neutron kinetic energy and if neutron scattering cross section is much smaller than geometrical cross section of the nanorod then the amplitude of neutron scattering can be calculated in perturbation theory. These approximations are valid for all cases of interest in the present work. In this case, the amplitude $F(\boldsymbol{q},\boldsymbol{l})$ of neutron scattering at a nanorod with a radius ρ and a length $2a$ with an axis along the unit vector $\boldsymbol{l}$ equals:

$$F(\boldsymbol{q},\boldsymbol{l}) = N_0 b \int_V d^3r \exp(i\boldsymbol{q}\cdot\boldsymbol{r}) = N_0 b \int\limits_{-a}^{a} dz \int\limits_0^{\rho} \rho' d\rho' \int\limits_0^{2\pi} d\phi \exp(iq_l z + iq_\rho \rho' \cos\phi) =$$

$$\frac{4\pi N_0 b}{q_l} \sin(q_l a) \int\limits_0^{\rho} \rho' d\rho' J_0(q_\rho \rho') = u_0 a \rho^2 \mathrm{sinc(q_l a)} \frac{\mathrm{J_1(q_\rho \rho)}}{\mathrm{q_\rho \rho}}, \qquad (1)$$

where sinc(x)=sin(x)/x, $u_0 = 4\pi N_0 b$ is potential of neutron interaction with the nanorod matter divided by a factor $\hbar^2/2m$ (m is the neutron mass, $\hbar$ is the reduced Planck constant), N_0 is the number of atoms in the unit volume of the nanorod, b is the length of neutron coherent scattering on a nucleus of the nanorod matter, $\boldsymbol{q} = \boldsymbol{k}_0 - \boldsymbol{k}$ is the transferred momentum, $\boldsymbol{k}_0$, $\boldsymbol{k}$ are momenta of the neutron before and after scattering, $q_l = \boldsymbol{q}\cdot\boldsymbol{l}$, $q_\rho = \sqrt{\boldsymbol{q}^2 - q_l^2}$, $J_0(x)$ and $J_1(x)$ are Bessel functions; and we also used the following expressions:

$$J_0(x) = \int_0^{2\pi} \frac{d\phi}{2\pi} \exp(ix\cos\phi), \qquad \int_0^x x' dx' J_0(x') = x J_1(x).$$

In this work we consider neutron scattering on diamond nanorods. The potential of interaction of a neutron with a nanorod matter is always assumed to be equal to 300 neV, as it is for neutron scattering at crystal diamond. This approximation is valid in the first order for nanospheres [24] as well as for nanorods [25], because their densities are close to the density of bulk diamond, and their shells are not very thick [26, 27], [28]. However, more accurate but also more bulky descriptions will be required for concrete reflector realizations. The refection is understood here as albedo, i.e. the probability of neutron reflection integrated over all backward angles. We will calculate albedo following works [29-31], and will remind below briefly the calculation method.

2. Method of albedo calculation

First we will define notations. A neutron moving along a solid angle Ω with the polar axis along the internal normal to the matter surface is defined by the state vector $|\Omega\rangle$. An angular distribution $P(\Omega)$ will be characterized by the state vector:

$$|P\rangle = \int_{4\pi} P(\Omega) d\Omega |\Omega\rangle. \tag{2}$$

The norm of this state $N_P = \int_{4\pi} P(\Omega) d\Omega$ is calculated by means of multiplication of eq. (2) from the left by a meter

$$|m\rangle = \int_{4\pi} d\Omega |\Omega\rangle,$$

using a natural relation $\langle\Omega||\Omega'\rangle = \delta(\Omega - \Omega')$. In particular, isotropic distribution of incident and reflected neutrons corresponds to the state

$$|P_{\rm is}\rangle = \int_{2\pi} \frac{|\cos\theta|}{\pi} d\Omega |\Omega\rangle. \tag{3}$$

Its norm is unity.

A scatterer, which transforms a neutron state $|\Omega'\rangle$ to a state $|\Omega\rangle$ with a probability $w(\Omega \leftarrow \Omega')$, is described by means of an operator

$$\hat{\boldsymbol{W}} = \int_{4\pi} |\Omega\rangle w(\Omega \leftarrow \Omega') \langle\Omega'| d\Omega d\Omega'.$$

A neutron from a state (2) is scattered into the state:

$$|P'\rangle = \hat{\boldsymbol{W}}|P'\rangle = \int_{4\pi} |\Omega\rangle w(\Omega \leftarrow \Omega') P(\Omega') d\Omega d\Omega' = \int_{4\pi} P'(\Omega) |\Omega\rangle d\Omega,$$

where

$$P'(\Omega) = \int_{4\pi} w(\Omega \leftarrow \Omega') P(\Omega') d\Omega'.$$

In order to calculate albedo R_D from a layer of powder with a finite thickness D, one first calculates albedo R_∞ from an infinitely thick layer. For this purpose, one splits a layer of small thickness ξ from the infinite one; scattering on this layer is calculated using perturbation theory, and it is presented in a form of a reflection $\hat{\boldsymbol{\rho}}_\xi$ and a transmission $\hat{\boldsymbol{\tau}}_\xi$ operators. In order to find the operator $\hat{\boldsymbol{R}}_\infty$ of reflection from an infinitely thick layer for incident neutrons in a state $|\Omega_0\rangle$, one has to know their distribution $|X_\xi\rangle = \hat{\boldsymbol{X}}_\xi |\Omega_0\rangle$ behind the thin layer. For the operator $\hat{\boldsymbol{X}}_\xi$ one could write a self-consisting equation

$$\hat{\boldsymbol{X}}_\xi = \hat{\boldsymbol{\tau}}_\xi + \hat{\boldsymbol{\rho}}_\xi \hat{\boldsymbol{R}}_\infty \hat{\boldsymbol{X}}_\xi, \tag{4}$$

which shows that $\hat{\boldsymbol{X}}_\xi$ is constructed from the transmission through the layer $\hat{\boldsymbol{\tau}}_\xi$ and from the contribution of $\hat{\boldsymbol{X}}_\xi$ itself, because a neutron behind the layer ξ is reflected from the infinite layer then is reflected ones again from a layer ξ, and returned to the infinitely thick layer, where the state $|X_\xi\rangle$ is formed together with the part characterized by the transmission $\hat{\boldsymbol{\tau}}_\xi$.

If we know $\hat{\boldsymbol{X}}_\xi$, we can write an equation for $\hat{\boldsymbol{R}}_\infty$:

$$\hat{\boldsymbol{R}}_\infty = \hat{\boldsymbol{\rho}}_\xi + \hat{\boldsymbol{\tau}}_\xi \hat{\boldsymbol{R}}_\infty \hat{\boldsymbol{X}}_\xi. \tag{5}$$

From (4) it follows

$$\hat{\boldsymbol{X}}_\xi = \left(\hat{\boldsymbol{I}} - \hat{\boldsymbol{\rho}}_\xi \hat{\boldsymbol{R}}_\infty\right)^{-1} \hat{\boldsymbol{\tau}}_\xi, \tag{6}$$

where $\hat{\boldsymbol{I}} = \int_{4\pi} |\Omega\rangle\langle\Omega| d\Omega$ is a unit operator. Substituting of (6) into eq. (5) gives

$$\hat{\boldsymbol{R}}_\infty = \hat{\boldsymbol{\rho}}_\xi + \hat{\boldsymbol{\tau}}_\xi \hat{\boldsymbol{R}}_\infty \left(\hat{\boldsymbol{I}} - \hat{\boldsymbol{\rho}}_\xi \hat{\boldsymbol{R}}_\infty\right)^{-1} \hat{\boldsymbol{\tau}}_\xi. \tag{7}$$

Operators $\hat{\boldsymbol{\rho}}_\xi$ and $\hat{\boldsymbol{\tau}}_\xi$ are related to macroscopic scattering cross sections:

$$\hat{\boldsymbol{\rho}}_\xi = \xi \hat{\boldsymbol{\Sigma}}_b, \qquad \hat{\boldsymbol{\tau}}_\xi = \hat{\boldsymbol{I}} + \xi \hat{\boldsymbol{\Sigma}}_f - \xi \Sigma_t \hat{\boldsymbol{S}}, \tag{8}$$

where

$$\hat{\boldsymbol{\Sigma}}_b = \int\limits_{\boldsymbol{n}\cdot\Omega<0} d\Omega \int\limits_{\boldsymbol{n}\cdot\Omega'>0} |\Omega\rangle \Sigma_s(\Omega \leftarrow \Omega') \frac{d\Omega'}{\cos\theta'} \langle\Omega'| = \int\limits_{\boldsymbol{n}\cdot\Omega>0} d\Omega \int\limits_{\boldsymbol{n}\cdot\Omega'<0} |\Omega\rangle \Sigma_s(\Omega \leftarrow \Omega') \frac{d\Omega'}{\cos\theta'} \langle\Omega'| \tag{9}$$

the operator of back scattering from the left or from the right,

$$\hat{\boldsymbol{\Sigma}}_f = \int\limits_{\boldsymbol{n}\cdot\Omega>0} d\Omega \int\limits_{\boldsymbol{n}\cdot\Omega'>0} |\Omega\rangle \Sigma_s(\Omega \leftarrow \Omega') \frac{d\Omega'}{\cos\theta'} \langle\Omega'| = \int\limits_{\boldsymbol{n}\cdot\Omega<0} d\Omega \int\limits_{\boldsymbol{n}\cdot\Omega'<0} |\Omega\rangle \Sigma_s(\Omega \leftarrow \Omega') \frac{d\Omega'}{\cos\theta'} \langle\Omega'| \tag{10}$$

is the operator of forward scattering from the left or right, $\Sigma_s(\Omega \leftarrow \Omega')$ is the differential macroscopic scattering cross section, $\Sigma_t = \Sigma_s + \Sigma_a$ is the total macroscopic cross section, consisting of the integral scattering Σ_s and absorption Σ_a cross sections, and

$$\hat{\boldsymbol{S}} = \int\limits_{2\pi} |\Omega\rangle \frac{d\Omega}{\cos\theta} \langle\Omega| \tag{11}$$

is an operator, which takes into account that the number of scatterers along the neutron path increases with increasing of the incidence angle.

At small value of ξ eq. (7) can be linearized and reduced to

$$\hat{\boldsymbol{R}}_\infty \hat{\boldsymbol{\Sigma}}_b \hat{\boldsymbol{R}}_\infty + \left(\hat{\boldsymbol{\Sigma}}_f - \Sigma_t \hat{\boldsymbol{S}}\right) \hat{\boldsymbol{R}}_\infty + \hat{\boldsymbol{R}}_\infty \left(\hat{\boldsymbol{\Sigma}}_f - \Sigma_t \hat{\boldsymbol{S}}\right) + \hat{\boldsymbol{\Sigma}}_b = 0. \tag{12}$$

We suppose that the distribution of reflected neutrons is isotropic, and represent the solution of (12) in the form

$$\hat{\boldsymbol{R}}_\infty = R_\infty \int\limits_{\boldsymbol{n}\cdot\Omega<0} |\Omega\rangle \frac{|\cos\theta|}{\pi} d\Omega \int\limits_{\boldsymbol{n}\cdot\Omega'>0} d\Omega' \langle\Omega'| = R_\infty |P_{\rm is}\rangle\langle m|. \tag{13}$$

Substitute it in (12) and multiply (12) from the left by $\langle m|$ and from the right by $|P_{\rm is}\rangle$. Then we get

$$R_\infty^2 \Sigma_b + 2R_\infty(\Sigma_f - \Sigma_t) + \Sigma_b = 0, \tag{14}$$

where

$$\Sigma_b = \int\limits_{\boldsymbol{n}\cdot\Omega<0} d\Omega \int\limits_{\boldsymbol{n}\cdot\Omega'>0} \Sigma_s(\Omega \leftarrow \Omega') \frac{d\Omega'}{2\pi} = \int\limits_{\boldsymbol{n}\cdot\Omega>0} d\Omega \int\limits_{\boldsymbol{n}\cdot\Omega'<0} \Sigma_s(\Omega \leftarrow \Omega') \frac{d\Omega'}{2\pi}, \tag{15}$$

$$\Sigma_f = \int\limits_{\boldsymbol{n}\cdot\Omega>0} d\Omega \int\limits_{\boldsymbol{n}\cdot\Omega'>0} \Sigma_s(\Omega \leftarrow \Omega') \frac{d\Omega'}{2\pi} = \int\limits_{\boldsymbol{n}\cdot\Omega<0} d\Omega \int\limits_{\boldsymbol{n}\cdot\Omega'<0} \Sigma_s(\Omega \leftarrow \Omega') \frac{d\Omega'}{2\pi} \tag{16}$$

are macroscopic cross sections of backward and forward scattering. Since $\Sigma_t = \Sigma_s + \Sigma_a = \Sigma_b + \Sigma_f + \Sigma_a$, then solution of eq. (12) can be represented in the form

$$R_\infty = \frac{\sqrt{\Sigma_a + 2\Sigma_b} - \sqrt{\Sigma_a}}{\sqrt{\Sigma_a + 2\Sigma_b} + \sqrt{\Sigma_a}} = \frac{\sqrt{1 + 2\Sigma_b/\Sigma_a} - 1}{\sqrt{1 + 2\Sigma_b/\Sigma_a} + 1}. \tag{17}$$

In order to calculate albedo from a wall of a finite thickness, one has to know a law of attenuation of neutron intensity in the matter. It follows from eq. (6). After linearization of it at small ξ, substitution of (13) and multiplication from left by $\langle m|$ and from the right by $|P_{\rm is}\rangle$ one gets

$$\langle m|\hat{\boldsymbol{X}}_\xi|P_{\rm is}\rangle = 1 - \xi/L \approx \exp(-\xi/L),$$

where

$$1/L = 2\sqrt{\Sigma_a + 2\Sigma_b}\sqrt{\Sigma_a} = 2\Sigma_a\sqrt{1 + 2\Sigma_b/\Sigma_a}. \tag{18}$$

Thus $\hat{\boldsymbol{X}}_z$ at a depth z can be represented as

$$\hat{\boldsymbol{X}}_z = |P_{\rm is}\rangle \exp(-z/L)\langle m|. \tag{19}$$

For calculating reflection $\hat{\boldsymbol{R}}_D$ and transmission $\hat{\boldsymbol{T}}_D$ from/through a layer of a thickness D we use eq-s. (4), (5) splitting a layer of a finite thickness D from the semiinfinite one. The equations then look:

$$\hat{\boldsymbol{X}}_D = \hat{\boldsymbol{T}}_D + \hat{\boldsymbol{R}}_D\hat{\boldsymbol{R}}_\infty\hat{\boldsymbol{X}}_D, \qquad \hat{\boldsymbol{R}}_\infty = \hat{\boldsymbol{R}}_D + \hat{\boldsymbol{T}}_D\hat{\boldsymbol{R}}_\infty\hat{\boldsymbol{X}}_D. \tag{20}$$

They can be resolved with respect to $\hat{\boldsymbol{R}}_D$ and $\hat{\boldsymbol{T}}_D$ for known $\hat{\boldsymbol{X}}_D$ and $\hat{\boldsymbol{R}}_\infty$. Assuming $\hat{\boldsymbol{R}}_D = R_D|P_{\rm is}\rangle\langle m|$, we get

$$R_D = R_\infty \frac{1 - \exp(-2D/L)}{1 - R_\infty^2 \exp(-2D/L)}. \tag{21}$$

It follows from (17) and (18) that in order to calculate R_D, which will be named below as simply R, one has to get macroscopic cross sections Σ_b and Σ_a, which are averaged over angles differential cross sections.

3. Calculation of macroscopic cross sections

From the scattering amplitude (1), one could calculate a differential cross section

$$d\sigma(\boldsymbol{q},\boldsymbol{l})/d\Omega = |F(\boldsymbol{q},\boldsymbol{l})|^2 = |u_0|^2a^2\rho^4\mathrm{sinc}^2(\mathrm{q_l a})\left|\frac{\mathrm{J_1(q_\rho\rho)}}{\mathrm{q_\rho\rho}}\right|^2. \tag{22}$$

Consider an angular distribution of scattered neutrons. The polar axis is directed along the wave vector $\boldsymbol{k}_0$ of the incidence wave, and the axis is in the plane of vectors ($\boldsymbol{k}_0$, $\boldsymbol{l}$) perpendicular to $\boldsymbol{k}_0$. where $\boldsymbol{l}$ is a unit vector along the rod axis. Then $\boldsymbol{k}_0 \cdot \boldsymbol{l} = k\cos\theta_0$ and

$$q_l = \boldsymbol{q}\cdot\boldsymbol{l} = k(\cos\theta_0 - \cos\theta_0\cos\theta_0 - \sin\theta\sin\theta_0\cos\phi), \tag{23}$$

where θ, ϕ are the angles of the vector $\boldsymbol{k}$ of the scattered wave. Eq. (22) can be integrated over angle ϕ. Taking into account the symmetry of eq. (23), we get

$$\frac{d}{d\cos\theta}\sigma(\theta,\theta_0) = |u_0|^2a^2\rho^4\int_0^\pi 2d\phi\ \mathrm{sinc}^2(\mathrm{q_l a})\left|\frac{\mathrm{J_1(q_\rho\rho)}}{\mathrm{q_\rho\rho}}\right|^2. \tag{24}$$

After multiplication of the differential cross section (24) by a number of nanorods N_1 in the unit volume, we get the macroscopic differential scattering cross section Σ:

$$\Sigma(\theta,\theta_0) = N_1 \frac{d}{d\cos\theta}\sigma(\theta,\theta_0) = A\int_0^{\pi} 2d\phi\ \mathrm{sinc}^2(\mathrm{q_l a})\left|\frac{\mathrm{J_1(q_\rho \rho)}}{\mathrm{q_\rho \rho}}\right|^2, \tag{25}$$

where

$$A = \gamma|u_0|^2 a\rho^2/2\pi,$$

and the value $\gamma = N_1V_1 = N_1 2\pi\rho^2 a$ characterizes a fraction of volume occupied by nanorod matter. In the following we will assume $\gamma = 0.1$. In order to describe precisely some concrete neutron nanorod reflectors we will need a more accurate model. The dimension of the coefficient A is 1/cm, and its value depends of nanorod parameters. In order to compare neutron cross sections for different nanorods, we introduce a convenient common dimensional coefficient

$$A_0 = \gamma|u_0|^2\rho_0^3/2\pi. \tag{26}$$

If nanorod radius is $\rho_0 = 10$ nm, then $A_0 = 3.4\ \mu m^{-1}$ (for diamond $1/\sqrt{u_0} = 8.27$ nm). The macroscopic cross section of neutron scattering (25) can be represented in the following form:

$$\Sigma(\theta,\theta_0) = 2A_0\frac{\overline{\rho}^3}{\beta}\int_0^{\pi} d\phi\ \mathrm{sinc}^2(\overline{\mathrm{q}}_\mathrm{l}\alpha)\left|\frac{\mathrm{J_1}(\overline{\mathrm{q}}_\rho\alpha\beta)}{\overline{\mathrm{q}}_\rho\alpha\beta}\right|^2, \tag{27}$$

with dimensionless parameters $\overline{q} = q/k$, $\alpha = ak$, $\beta = \rho/a$, $\overline{\rho} = \rho/\rho_0$. The macroscopic differential cross section $\Sigma(\theta,\theta_0)$ of scattering of a neutron on powder of nanorods, in units $2A_0\overline{\rho}^3/\beta$, is shown in Fig. 1 ($a = 1000$ nm) and in Fig. 2 ($a = 10$ nm), as a function of the neutron scattering angle θ provided the neutron incidence angle θ_0 equals 0, $\pi/4$ and $\pi/2$, the nanorod radius = 0=10 nm, and for the neutron velocity $v = 450$ m/s.

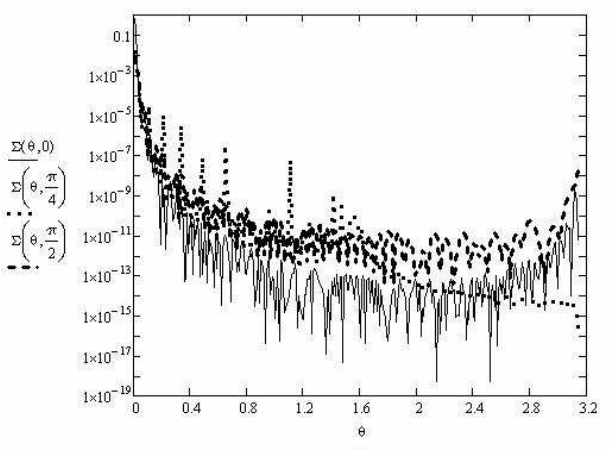

Figure 1. Dimensionless differential cross section $\Sigma(\theta,\theta_0)$ of the neutron scattering on nanorods as a function of the neutron scattering angle θ and the neutron incidence angle θ_0. The angles are measured relative to the nanorod axis, $v = 450$ m/s, $a = 1000$ nm.

Angles are given in radians. Cross sections of neutron scattering on nanorods with the half-length equals radius $a = \rho$ are approximately equal to the cross section of neutron scattering on spherical nanoparticles of equal radius, therefore we will use in the following for simplicity the same analytical expressions for qualitative comparison of results for long nanorods and

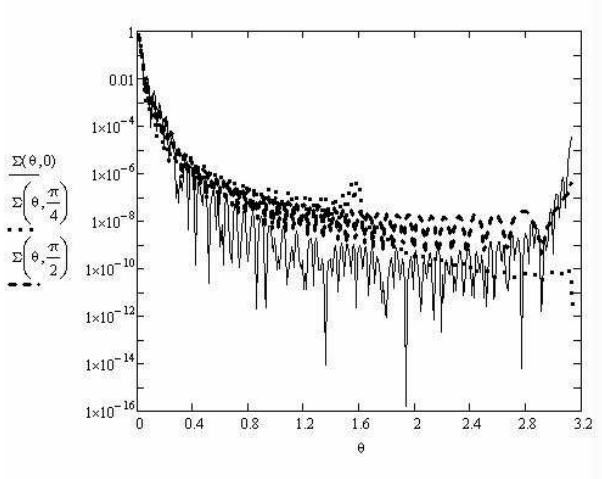

Figure 2. The same as in Fig. 1, but for the nanorod half-length of $a = \rho = 10$ nm.

for spherical nanoparticles. The average angle of neutron scattering on nanoparticles is equal approximately to the ratio of neutron wavelength to nanoparticle size. Thus, neutrons scatter on long nanorods to smaller angles (Fig. 1) then they scatter on short nanorods (Fig. 2). And the cross sections of neutron scattering to the zero angles are equal to each other as well as to $\pi/2$. It is interesting to note some increase of cross sections for backscattering, which is particularly visible for nanorods. It is useful to consider separately the cases of chaotic and ordered orientation of long nanorods in reflectors. In section 4 we consider the reflection of isotropic VCN flux from a reflector built of chaotically oriented nanorods; in section 5 we analyze the reflection of CN from a reflector built of nanorods with the axis parallel to the reflector surface while they are isotropically oriented over the azimuth angle.

4. Cross section of backward neutron scattering on chaotically oriented nanorods

To find scattering of neutrons on isotropically distributed nanorods one can average (22) over directions $\boldsymbol{l}$ for a given vector $\boldsymbol{q}$, which is chosen as a polar axis. In that case $\overline{q}_l = \overline{q}\cos\theta_l$ and $\overline{q}_\rho = \overline{q}\sin\theta_l$, and one should average (22) over angle θ_l of nanorod orientation. After averaging and multiplication by particle density N_1 we get in units $A_0\overline{\rho}^3/\beta$:

$$\langle d\Sigma_s(\boldsymbol{q},\boldsymbol{l},\alpha,\beta)/d\Omega\rangle = \int_0^1 dx\ \mathrm{sinc}^2(\mathrm{x}\overline{\mathrm{q}}\alpha)\left|\frac{\mathrm{J}_1(\sqrt{1-\mathrm{x}^2}\overline{\mathrm{q}}\alpha\beta)}{\sqrt{1-\mathrm{x}^2}\overline{\mathrm{q}}\alpha\beta}\right|^2. \tag{28}$$

In order to calculate the neutron albedo from powder of nanorods, we should know the cross section of backward scattering relative to the normal to the powder surface. We define the normal to surface to be the polar axis directed towards matter. Then the $\overline{q}$ for backward scattered neutrons is

$$\overline{q} = \sqrt{2(1+\cos\theta\cos\theta_0 - \sin\theta\sin\theta_0\cos\phi)}, \tag{29}$$

where θ and ϕ are the scattered neutron angles, and axis is in the incidence plane. We denote $y = \cos\theta\cos\theta_0 = \sin\theta\sin\theta_0\cos\phi$, integrate over $d\Omega = d\phi d\cos\theta$, average over directions θ_0 of incidence neutrons, and present this expression in the form

$$\Sigma_s(\alpha,\beta) = \int_{-1}^1 dy\delta(y-\cos\theta\cos\theta_0+\sin\theta\sin\theta_0\cos\phi)d\Omega d\cos\theta_0 S(y,\alpha,\beta), \tag{30}$$

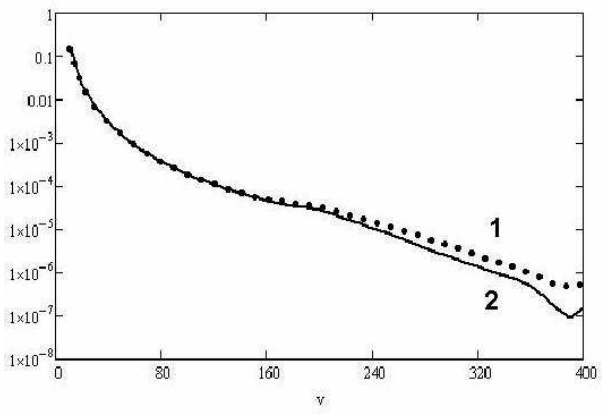

Figure 3. Dimensionless macroscopic cross section of neutron backward scattering $\Sigma_b(\alpha,\beta)/\beta$ on powder of long nanorods ($\Sigma bl(v)$) with the half-length of $a = 1000$ nm and on powder of short nanorods ($\Sigma bs(v)$) with the half-length of $a = 10$ nm. In both cases, the nanorod radius equals $\rho = 10$ nm.

where

$$S(y,\alpha,\beta) = \int_0^1 dx\ \mathrm{sinc}^2(\mathrm{x}\sqrt{2(1+\mathrm{y})}\alpha)\left|\frac{\mathrm{J}_1(\sqrt{1-\mathrm{x}^2}\sqrt{2(1+\mathrm{y})}\alpha\beta)}{\sqrt{1-\mathrm{x}^2}\sqrt{2(1+\mathrm{y})}\alpha\beta}\right|^2. \tag{31}$$

After integration of eq. (30) over $d\phi$ we get

$$\Sigma_b(\alpha,\beta) = \int_{-1}^1 dy I(y) S(y,\alpha,\beta), \tag{32}$$

where

$$I(y) = \int_0^1 d\cos\theta \int_0^1 d\cos\theta_0 \frac{\Theta(\sin^2\theta\sin^2\theta_0 > (\cos\theta\cos\theta_0 - y)^2)}{\sin^2\theta\sin^2\theta_0 - (\cos\theta\cos\theta_0 - y)^2}, \tag{33}$$

and Θ is the step-function, which is equal to 1 provided inequality in its argument, and is equal zero otherwise. Function I(y) is calculated in (A4). It is equal to

$$I(y) = \pi\Theta(y>0) - \arctan\left(\frac{\sqrt{1-y^2}}{y}\right). \tag{34}$$

Fig. 3 shows the dimensionless macroscopic cross section $\Sigma_b(\alpha,\beta)$ of neutron scattering as a function of its velocity v for powder of nanorods with the half-length $a = 1000$ nm, and $a = 10$ nm.

5. Absorption cross section

The total cross section is defined by the imaginary part of the forward scattering amplitude (1):

$$\Im(F(\boldsymbol{q},\boldsymbol{l}))_{q=0} = u_0'' a\rho^2/2 = N_0 k\sigma_l(k) a\rho^2/2, \tag{35}$$

and it actually describes absorption, as scattering in the perturbation theory is not included in this expression. The macroscopic cross section of absorption is equal:

$$\Sigma_a(k) = \frac{4\pi}{k} N_1 \Im(F(\boldsymbol{q},\boldsymbol{l}))_{q=0} = \frac{4\pi}{2k} N_1 N_0 k\sigma_l(k) a\rho^2 = \frac{\gamma u_0^2 \rho_0^3}{2\pi}\frac{k_T\sigma_l(k_T)}{2kbu_0\rho_0^3} = A_0\frac{C\overline{\rho}}{\alpha\beta}, \tag{36}$$

where

$$C = \frac{k_T \sigma_l(k_T)}{2bu_0\rho_0^2} = \frac{\sigma_l(k_T)}{2bk_T(u_0/k_T^2)\rho_0^2}. \tag{37}$$

T denotes the ambient temperature, $\rho_0 = 10$ nm, $b = 6.65$ fm, and $u_0/k_T^2 = E_c/E_T = 12 \times 10^{-6}$. In the following, we will consider two cases of particular interest:

(i) Nanoparticles at a so small temperature that neutron heating in powder can be neglected, and also neutron cooling would even increase albedo. Also hydrogen in powder is substituted by deuterium, and neutron absorption in deuterium can be neglected. It is the case of most efficient reflector, which could be built using the principle considered in the present article. In this case, absorption cross section is attributed to one carbon atom; it is equal $\sigma_l(kT) = 0.0035$ bn, and $C = C_0 = 6.28 \times 10^{-7}$.

(ii) Nanoparticles at the ambient temperature, with a realistic admixture of hydrogen. As nanopowder reflectors are most efficient for small neutron energy compared to the ambient temperature (energy), then inelastic neutron scattering is equivalent to neutron loss. And inelastic scattering is governed by a relatively small admixture of hydrogen in powder. As shown in [32], the minimum admixture of hydrogen atoms, which can be achieved by means of heating and degassing of powder, corresponds to the following composition $C_{12.4+0.2}H$, and the total cross section of neutron scattering on the atom of residual hydrogen at the ambient temperature, measured for neutrons with the wavelength of 4.4 Å, equals 108 ± 2 bn. In this case, the efficient cross section per one atom of the composition is $\sigma_l(kT) = 3.56$ bn. Thus the most pessimistic estimation gives $C = C_a = 5.2 \times 10^{-4}$. Neutron albedo from an infinitely thick layer of nanorods is equal [25-27] (17):

$$R_\infty(\alpha, \beta, \overline{\rho}, C) = \frac{\sqrt{1 + Q(\alpha, \beta, \overline{\rho}, C)} - 1}{\sqrt{1 + Q(\alpha, \beta, \overline{\rho}, C)} + 1}, \tag{38}$$

where

$$Q(\alpha, \beta, \overline{\rho}, C) = \frac{2\Sigma_b}{\Sigma_a} = \frac{2}{C}\Sigma_b(\alpha, \beta)\frac{\alpha\beta}{\overline{\rho}}. \tag{39}$$

Calculations of neutron albedo from an infinitely thick layer of nanorods, as a function of the velocity v of incidence neutrons for long ($a = 1000$ nm) and short ($a = 10$ nm) nanorods, show that neutron albedo from nano-structured powder for the neutron velocity of $v = 400$ m/s is significantly larger than the coefficient of neutron reflection 5×10^{-9} from continuous matter.

Besides the reflection from infinite matter, albedo is characterized also by the exponential attenuation in matter $\exp(-x/L)$, i.. by the attenuation length (18):

$$1/L = 2\sqrt{\Sigma_a + 2\Sigma_b}\sqrt{\Sigma_a} = 2\Sigma_a\sqrt{1 + Q(\alpha, \beta, \overline{\rho}, C)} = L_0^{-1}(C)\kappa^{-1}(\alpha, \beta, \overline{\rho}, C). \tag{40}$$

Substitution of (36) gives

$$L_0^{-1}(C) = 2CA_0, \qquad \kappa(\alpha, \beta, \overline{\rho}, C) = \frac{\alpha\beta}{\overline{\rho}\sqrt{1 + Q(\alpha, \beta, \overline{\rho}, C)}}. \tag{41}$$

Consider now the neutron reflection from a layer of nanopowder with a finite thickness d. Albedo from such a layer is defined by formula:

$$R(d, \alpha, \beta, \overline{\rho}, C) = R_\infty(\alpha, \beta, \overline{\rho}, C)\frac{1 - \exp(-2d/L(\alpha, \beta, \overline{\rho}, C))}{1 - R_\infty^2(\alpha, \beta, \overline{\rho}, C)\exp(-2d/L(\alpha, \beta, \overline{\rho}, C))}. \tag{42}$$

Fig. 4 shows dependence R(v) for the nanopowder thickness of $d = 3$ cm for long and short nanorods with the neutron loss coefficients C_0 and C_a. The figure shows that the neutron albedo from a sufficiently thin layer of nanoparticles is higher by 6-7 orders of magnitude than neutron reflection from continuous matter.

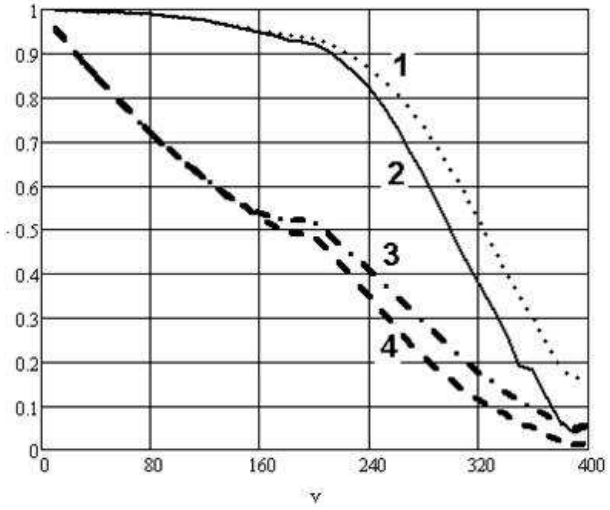

Figure 4. Albedo from powder of nanorods of length: 1, 3) $a = 10$ nm; 2, 4) $a = 1000$ nm; with absorption parameter C equal to 1. 2) C_0; 3, 4) C_a. In all cases, the nanorod radius equals $\rho = 10$ nm. It is seen that quasi spherical nanorods reflect better than long ones.

6. Axes of nanorods are oriented parallel to the interface

Now consider the case when nanorods are oriented parallel to the powder surface. We define the polar axis along the normal to the interface directed towards matter, and axis in the incidence plane then:

$$\overline{q}_l = \sin\theta_0 \cos\chi - \sin\theta\cos(\phi - \chi), \tag{43}$$

where χ is the azimuth angle of the nanorod orientation, and θ, ϕ are scattering angles. Then

$$\overline{q}_\rho = \sqrt{2(1 + \cos\theta\cos\theta_0 - \sin\theta\sin\theta_0\cos\phi) - (\sin\theta_0\cos\chi - \sin\theta\cos(\phi - \chi))^2}. \tag{44}$$

After averaging over nanorod orientation, integrating over backward scattering angles, and averaging over angular distribution of incident neutrons, we get

$$\Sigma_b(\alpha, \beta, \overline{\rho}) = \int_0^1 dx \int_0^1 dy \Sigma_{b,\theta}(x, y, \alpha, \beta, \overline{\rho}), \tag{45}$$

where

$$\Sigma_{b,\theta}(x, y, \alpha, \beta, \overline{\rho}) = \frac{\overline{\rho}^3}{\beta} \int_0^{2\pi} d\phi \int_0^{2\pi} \frac{d\chi}{2\pi} \mathrm{sinc}^2(\alpha \overline{\mathrm{q}}_\mathrm{l}(\mathrm{x}, \mathrm{y}, \alpha, \beta)) \left| \frac{\mathrm{J}_1(\alpha\beta\, \overline{\mathrm{q}}_\rho(\mathrm{x}, \mathrm{y}, \alpha, \beta))}{\alpha\beta\, \overline{\mathrm{q}}_\rho(\mathrm{x}, \mathrm{y}, \alpha, \beta)} \right|^2. \tag{46}$$

Numerical integration of (46) shows the macroscopic cross section of neutron backward scattering as a function of $x = \cos\theta$ for given values of $y = \cos\theta_0$. This dependence for long nanorods ($\beta = 0.01$) at $\overline{\rho} = 1$, the neutron velocity $v = 450$ m/s and two values of cosine of the incident angle $y = 0,3$ and $y = 0,8$ is shown in fig. 5. One can see the peaks in the vicinity of $\cos\theta = \cos\theta_0$, which correspond to quasi-specular reflection. For isotropic distribution of nanorods the quasi specular reflection will possibly appears only after introduction of an interference between the waves scattered on different grains.

Integration in (45) and substitution into albedo formulas gives the results shown in fig. 6. Here we show neutron albedo from a layer with the thickness of 3 cm as a function of the

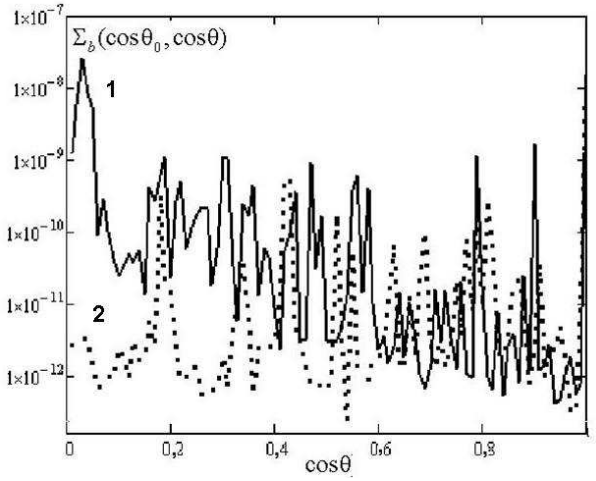

Figure 5. Dependence $\Sigma_{b\theta}(\cos\theta_0, \cos\theta, \alpha, \beta, \overline{\rho})$ on $\cos\theta$ at 1) $\cos\theta_0 = 0.3$; 2) $\cos\theta_0 = 0.8$ – for long nanorods: $\beta = 0.01$, $\rho = 10$ nm and for $v = 450$ m/s.

neutron speed v, m/s; the layer consists of long and short nanorods oriented along the interface but isotropically with respect to the azimuth around the interface normal. Albedo is calculated for small and large content of hydrogen. It is seen that albedo from long nanorods is higher than that from short quasi spherical ones. The results of calculations are in good agreement with the experimental observations for v in the range 50-150 m/s [11].

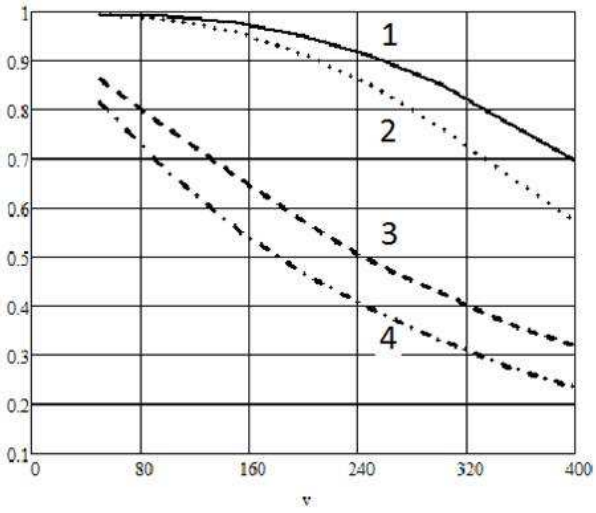

Figure 6. . Albedo $R_d(v)$ from powder layer of thickness $d = 3$ cm composed of: 1, 3) long ($a = 1000$ nm) and 2,4) short ($a = 10$ nm) nanorods with the radius $\rho = 10$ nm; for two loss coefficients 1, 2) $C = C_0 = 6.28 \times 10^{-7}$ and $C = C_a = 5.2 \times 10^{-4}$ as a function of neutron velocity v, m/s.

7. A problem of accounting for the real angular distribution

We have assumed above that albedo is calculated for the isotropic distribution of reflected and incident neutrons. How would change the results, if one does not keep these assumptions? In

order to answer this question, one has to solve eq. (12) in its general form. It is an extremely complex problem involving a non-linear integral equation. It can be simplified, provided a natural assumption that all functions depend only on cosines of incidence and reflected angles. Then the integral equation can be reduced by discretization to an algebraic matrix equation of the second order of the form

$$\hat{\boldsymbol{Z}}\hat{\boldsymbol{A}}\hat{\boldsymbol{Z}} + \hat{\boldsymbol{B}}\hat{\boldsymbol{Z}} + \hat{\boldsymbol{Z}}\hat{\boldsymbol{C}} + \hat{\boldsymbol{D}} = 0. \tag{47}$$

However solving such a quadratic matrix algebraic equation also is a complex problem. In fact, a quadratic matrix equation for the matrix $N \times N$ is equivalent in the general case to a polynomial equation with the power $2N^2$. And even, if one calculates numerically all its roots, there will stay a problem of choosing a proper set of roots. However it is possible to shed light on a role of scattering anisotropy by suggesting solution of eq. (12) not in the purely isotropic form (13), but as a combination of isotropic and specular distributions as shown in (47),

$$\hat{\boldsymbol{R}}_\infty = R_\infty \int_{\boldsymbol{n}\Omega<0} |\Omega\rangle \frac{|\cos\theta|}{\pi} d\Omega \int_{\boldsymbol{n}\Omega>0} d\Omega' \langle\Omega'| + \int_{\boldsymbol{n}\Omega<0} d\Omega |\Omega\rangle \boldsymbol{n}_{\Omega<0} f(\Omega) \langle\Omega| \boldsymbol{n}_{\Omega>0}, \tag{48}$$

where the specular part is presented by the diagonal term. This option will be considered in another work.

8. Conclusion

In the present theoretical work we considered a possibility to increase efficiency of nano-structured reflectors of slow neutrons by means of substituting spherical nanoparticles by nanorods. We show that albedo of VCN from powder of disordered nanorods is smaller than the albedo from powder of nanospheres. However, albedo of VCN and quasi-specular reflection of CN from powder of nanorods oriented parallel to the reflector surface exceed respective values for powder of nanospheres.

Acknowledgments
The authors are sincerely grateful for useful discussions and critics to our colleagues V A Artem'ev, E V Lychagin, A Yu Muzychka, and A V Strelkov.

Appendix A. Calculation of the integral (19)

Denote $\cos\theta = v$, $\cos\theta_0 = u$. Then integral (19) is presented in the form

$$I(y) = \int_0^1 du \int_0^1 dv \frac{\Theta(1 - u^2 - v^2 + u^2v^2 > y^2 - 2yuv)}{1 - u^2 - v^2 + u^2v^2 - y^2 + 2yuv} = \int_0^1 du I_1(u, y), \tag{A.1}$$

where integral $I_1(u, y)$, after variable substitution $x = (v - uy)/sqrt1 - u^2 sqrt1 - y^2$ is reduced to

$$I_1(u,y) = \int\limits_{-x_1(u,y)}^{x_2(u,y)} dx \frac{\Theta(x^2 < 1)}{\sqrt{1-x^2}} = \frac{\pi}{2}\left(1 + \Theta\left(u > \sqrt{1-y^2}\right)\frac{|y|}{y}\right) + \\ + \arcsin(x_1(u,y))\Theta\left(u < \sqrt{1-y^2}\right). \tag{A.2}$$

Limits of integration in (2) are

$$x_1(u,y) = \frac{uy}{\sqrt{(1-u^2)(1-y^2)}}, \qquad x_2(u,y) = \frac{1-uy}{\sqrt{(1-u^2)(1-y^2)}}. \tag{A.3}$$

Modulus of these limits have to be smaller than unity, but $x_2(u,y) > 1$ for any values of u and y, therefore the upper limit, due to the inequality in the integral, has to be replaced by unity. The lower limit, $|x_1(u,y)| \leq 1$, only when $u \leq u_1(y) = \sqrt{1-y^2}$. If $u > u_1(y) = \sqrt{1-y^2}$, then modulus of the lower limit has to exceed unit and thus the lower limit should be replaced by -1 or +1, which depends on the sign of y. Accounting for all these conditions leads to (A2). Substitution of (2) into (1) and integration by parts of the term containing arcsin provides the final result:

$$I(y) = \int_0^1 du I_1(u,y) = \frac{\pi}{2}\left[1 + (1+\sqrt{1-y^2})\frac{y}{|y|}\right] + \sqrt{1-y^2})\frac{y}{|y|}\frac{\pi}{2} -$$
$$- \int_0^{\sqrt{1-y^2}} \frac{yudu}{(1-u^2)\sqrt{1-u^2-y^2}} = \pi\Theta(y>0) - \arctan\left(\frac{\sqrt{1-y^2}}{y}\right). \qquad \text{(A.4)}$$

References

[1] Luschikov V I, Pokotilovskiy Yu N, Strelkov A V et al 1969 Observation of ultracold neutrons *JETP Lett.* **9** 23

[2] Ignatovich V K 1990 *The Physics of Ultracold Neutrons* (Oxford, UK: Clarendon Press)

[3] Golub R, Richardson D J, and Lamoreux S K 1991 *Ultracold Neutrons* (Bristol: Higler)

[4] Mezei F 1976 Novel polarized neutron devices - supermirror and spin component amplifier *Commun. Phys.* **1** 81

[5] Maruyama R, Yamazaki D, Ebisawa T et al 2007 Development of neutron supermirrors with large critical angle, *Thin Solid Films* **515** 5704

[6] Carron I and Ignatovich V 2003 Algorithm for preparation of multilayer systems with high critical angle of total reflection *Phys. Rev.* A **67** 043610

[7] Amaldy E, and Fermi E 1936 On the absorption and the diffusion of slow neutrons, *Phys. Rev.* **50** 899

[8] Nesvizhevsky V V 2002 Interaction of neutrons with nanoparticles, *Phys. At. Nucl.* **65** 400

[9] Artem'ev V A 2006 Estimation of neutron reflection from nanodispersed materials, *At. Energy* **101** 901

[10] Nesvizhevsky V V, Lychagin E V, Muzychka A Yu et al 2008 The reflection of very cold neutrons from diamond powder nanoparticles, *Nucl. Instrum. Meth.* A **595** 631

[11] Lychagin E V, Muzychka A Yu, Nesvizhevsky V V et al 2009 Storage of very cold neutrons in a trap with nano-structured walls, *Phys. Lett.* B **679** 186

[12] Lychagin E V, Muzychka A Yu, Nesvizhevsky V V et al 2009 Coherent scattering of slow neutrons at nanoparticles in particle physics experiments, *Nucl. Instrum. Meth.* A **611** 302

[13] Nesvizhevsky V V, Cubitt R, Lychagin E V et al 2010 Application of diamond nanoparticles in low-energy neutron physics, *Materials* **3** 1768

[14] Cubitt R, Lychagin E V, Muzychka A Yu et al 2010 Quasi-specular reflection of cold neutrons from nano-dispersed media at above-critical angles, *Nucl. Instrum. Meth.* A **622** 182

[15] Nesvizhevsky V V 2011 Reflectors for VCN and applications of VCN *Rev. Mexicana Fiz.* **57** 1

[16] Golub R, and Pendlebury J M 1975 Super-thermal sources of ultra-cold neutrons, *Phys. Lett.* A **53** 133

[17] Schmidt-Wellenburg Ph, Andersen K N, Courtois P et al 2009 Ultra-cold neutron infrastructure for the gravitational spectrometer GRANIT, *Nucl. Instrum. Meth.* A **611** 267

[18] Baessler S, Beau M, Kreuz M et al 2011 The GRANIT spectrometer, *Comp. Rend. Phys.* **12** 707

[19] Luschikov V I, and Frank A I 1978 Quantum effects occuring when ultracold neutrons are stored on a plane, *JETP Lett.* **28** 559

[20] Nesvizhevsky V V, Boerner H G, Petukhov A K et al 2002 Quantum states of neutrons in the Earth's gravitational field, *Nature* **415** 297

[21] Nesvizhevsky V V, Voronin A Yu, Cubitt R et al 2010 Neutron whispering gallery, *Nature Phys.* **6** 114

[22] Nesvizhevsky V V 2010 Near-surface quantum states of neutrons in the gravitational and centrifugal potentials, *Physics-Uspekhi* **53** 645

[23] Nesvizhevsky V V 2012 Gravitational quantum states of neutrons and the new GRANIT spectrometer, *Mod. Phys. Lett.* A **27** 1230006

[24] de Carli P S, and Jamieson J C 1961 Formation of diamond by explosive shock, *Science* **133** 1821

[25] Irifune T, Kurio A, Sakamoto S et al 2003 Materials - ultrahard polycrystalline diamond from graphite, *Nature* **421** 599

[26] Aleksenskii A E, Baidakova M V, Vul' A Y et al 1999 The structure of diamond nanoclusters, *Phys. Solid State* **41** 668

[27] Dolmatov V Yu 2007 Detonation nanodiamonds: synthesis, structure, properties and applications, *Uspekhi Khimii* **76** 375
[28] Dubrovinskaia N, Dubrovinsky L, Crichtion W et al 2005 Aggregated diamond nanorods, the densest and least compressible form of carbon, *Appl. Phys. Lett.* **87** 083106
[29] Ignatovich V K, and Shabalin E P 2007 Algebraic method for calculating a neutron albedo, *Phys. At. Nucl.* **70** 265
[30] Ignatovich V K 2006 *Neutron optics* (M.: Nauka Fizmatlit)
[31] Utsuro M, and Ignatovich V 2010 *Handbook of neutron optics* (Berlin: Wiley-VCH)
[32] Krylov A R, Lychagin E V, Muzychka A Yu et al 2011 Study of bound hydrogen in powders of diamond nanoparticles, *Crystallography Rep.* **56** 102